Laboratory tests of scour at a seawall

J Sutherland[1], C Obhrai[1], RJS Whitehouse[1] and AMC Pearce[2]

[1] HR Wallingford Ltd., Wallingford, Oxfordshire, OX10 8BA, UK
[2] University of Southampton, Southampton, SO17 1BJ, UK

Published in the Journal of…

Abstract

A set of medium-scale laboratory tests of wave-induced scour at seawalls has been performed in a flume at HR Wallingford. The methodology is presented along with test conditions and summarized results. The scour depth at the toe of the seawall is highly dependent on the form of wave breaking onto the structure. Sea states where waves plunge directly onto the wall generate jets of water that may penetrate to the seabed and cause a local scour hole immediately adjacent to the seawall. This is a different scouring mechanism to that observed in deeper water and is also absent when the seawall is well within the surf zone and most of the large waves have broken before they reach the seawall. Theoretical limitations are discussed.

1. Introduction

Toe scour is believed to be the most common cause of seawall failure in the UK [1] yet some of the empirical predictors of toe scour derived from laboratory tests give results with opposite dependence on relative depth [2, 3, 4]. Moreover many of the existing laboratory experiments on scour in front of seawalls were performed at relatively small scales, leading to tests dominated by bedload transport [2]. The pattern of sediment erosion and accretion varies with the mode of sediment transport, so bedload transport gives a different bed profile to suspended load transport [2, 5].

In many circumstances scour problems in the field will be dominated by suspended sediment transport. The results from physical model results are likely to be misleading unless the most important scaling parameters are satisfied. Therefore, laboratory tests should be done with a justification of the scale used and with an awareness of the ambiguities that have arisen in previous experiments done at small-scale. As a minimum it is recommended that the dominant transport mode (bedload or suspended) is reproduced in the laboratory. In many cases when considering sand beaches this will require suspended sediment transport to be produced in the laboratory for a significant proportion of the time. This will require experiments to be performed at a medium to large scale.

A number of wave flume experiments on toe scour at seawalls that were conducted at medium to large-scale, used fine sand and were conducted with irregular waves have been identified and their results collated. This database has been extended and gaps in it filled by devising and performing a set of medium-scale experiments of toe scour in front of smooth seawalls in a new wave flume in the Froude Modelling Hall at HR Wallingford. The laboratory tests looked at the longshore-uniform case of normal wave incidence only.

2. Prediction of suspension

Scaling rules have been developed for bedload [6] and suspended load [7] tests. In cases where suspended sediment is predominant the Shields parameter does not have to be preserved [7, 8] as wave breaking and turbulence are more dominant mechanisms in determining sediment mobility than the wave shear stress. In this case an undistorted model with Froude scaling using the same value of the Dean fall speed parameter in model and prototype is recommended. The Dean fall speed parameter, D_{ws}, is given by:

$$D_{ws} = \frac{H_s}{w_s T_p} \tag{1}$$

Here H_s is the significant wave height, w_s is the fall speed of the median sediment and T_p is the spectral peak wave period. Various formulae have been derived that distinguish between suspended and bedload hydrodynamic regimes. The following criterion has been proposed [9] for the initiation of suspension under waves:

$$\frac{U_w - U_{cr}}{w_s} \geq 16.5 \tag{2}$$

where U_w is the maximum value of orbital velocity at the bed and U_{cr} is the critical velocity for incipient sediment transport.

Simple Froude scaling rules exist for the fall velocities of both small and large particles (if the same density material is used in model and prototype) but not for intermediate values. Therefore, Equation 3 [10] was used to determine the sediment fall speed, w_s as:

$$w_s = \frac{\nu}{d}\left[\left(10.36^2 + 1.049 D_*^3\right)^{1/2} - 10.36\right] \tag{3}$$

Where D_* is the dimensionless grain size given by:

Funded by the UK Department for Environment, Food and Rural Affairs (Defra) under the joint Defra/Environment Agency R&D project FD1927

$$D_* = \left[\frac{g(s-1)}{\nu^2}\right]^{1/3} d \tag{4}$$

.

Here ν is the kinematic viscosity, d is the grain diameter, g is gravitational acceleration and $s=\rho_s/\rho$ is the relative density with ρ_s the sediment density and ρ the water density.

The critical velocity for incipient transport, U_{cr} [11] is given by Equation 5:

$$U_{cr} = \left[0.118 g(s-1)\right]^{2/3} d^{1/3} T^{1/3} \tag{5}$$

The maximum near-bed wave velocity, U_w, can be calculated from linear theory for a representative wave. Substituting U_w, U_{cr} and w_s back into Equation 2 determines if a test should generate suspended sediment transport and was used in the planning of the test series.

3. Existing datasets

Results from the tests reported here are comparable to those from the following datasets on toe scour that had suspended sediment transport and were conducted with irregular waves. The comparisons will be performed elsewhere, however.

Xie [9] included a number of tests that generated scour in a flat bed in front of a vertical seawall that were in the suspension mode. Most of the tests used regular waves but three irregular wave tests were also conducted in suspension mode. Scour profiles were provided from two of those tests.

Fowler [3] performed mid-scale (wave heights between 0.2 and 0.3m) laboratory tests of the scouring of a 1:15 sloping sand bed in front of a vertical wall, which was always placed close to the intersection of the beach and mean water line. All 18 irregular wave tests were conducted in the ranges $-0.011<h_t/L_0<0.025$ and $0.015<H_s/L_0<0.040$ where h_t is the initial water depth at the toe of the seawall and L_o is the linear theory deep water wavelength. Ottawa sand, with d_{50}=0.13mm and a specific gravity of 2.65 was used in all cases.

The SUPERTANK Data Collection Project was performed at the O.H. Hinsdale Wave Research Laboratory (WRL), Oregon State University [12, 13]. The WRL flume is 104.2m long, 3.66m wide and 4.57m (15 feet) deep. The beach was made of very well-graded sand trucked from the Oregon coast with a median diameter, d_{50} = 0.22mm. Waves were run in relatively short bursts to provide data for numerical model calibration. Only in one toe scour test, ST_C0, were about 3,000 waves of the same spectrum run.

4. Experimental setup

The new tests were performed in a 45m long wave flume at HR Wallingford [14, 15]. The internal cross-section of the flume is 1.2m wide by 1.7m high. Waves were generated using a piston-type wavemaker with a maximum stroke of ±0.6m and a maximum operating depth of 1.4m. The wavemaker has an absorption system for absorbing wave energy reflected from the seawalls. The test setup had a 19.2m long 1:30 smooth concrete slope from the flume floor up to an elevation of 0.64m. The test section was a 5.14m long sand bed filled with Redhill 110 sand. The sand bed was 0.3m deep at the offshore end. Tests 1 to 14 all started from a screeded 1:30 slope. The sand bed level at the wall was therefore approximately 0.80m above the flume floor. Tests 15-34 started from a screeded 1:75 slope where the sand bed level at the wall was approximately 0.7m above the flume floor.

Redhill 110 sand has typically 98.80% SiO_2, 0.09% Fe_2O_3, 0.21% Al_2O_3 and 0.14% loss on ignition. The results of a sieve analysis of Redhill 110 are shown in Table I. Given that d_n is the sieve size that n percent of the sand by weight passes through, common percentiles are d_{16} = 0.087mm, d_{50} = 0.111mm and d_{84} = 0.154mm. Settling velocities are also given using (3) and (4) for fresh water (salinity = 0) at a typical temperature in the tests of 11ºC, giving calculated density of water ρ = 999.5kgm^{-3} and a kinematic viscosity v = 1.27×10^{-6}m^{2}s^{-1}. In addition, a sediment density ρ_s = 2650kgm^{-3} was assumed – appropriate for silica sand.

Waves were measured by 10 wave gauges. A group of 4 wave gauges was situated over the flat flume bed before the start of the beach slope and were used to separate out incident and reflected wave spectra using a least-squares technique. A second group of 4 wave gauges was situated at the offshore end of the sand bed to separate out incident and reflected wave spectra over the sand bed. Variations in the standard deviation in the surface elevation at these gauges could also be used to provide information on the partial standing wave pattern in front of the seawall. A further two wave gauges were placed 1.00m and 0.10m in

front of the seawall, where local variations in the water level were greater due to the stronger partial standing wave pattern.

The profile of the sand bed was measured using the touch sensitive, 2D bed profiling system developed at HR Wallingford. The profiler consists of a probe which can move up and down and is mounted on a carriage which moves horizontally along a support beam. On the bottom of the probe is a sensor which consists of a lightweight "finger" that can move freely up and down inside a 20mm cylinder. The cylinder rests either on a small ball that is pulled along the bed by a lever arm mounted on the probe or on a foot that takes small steps (see Fig. 1).

The resolution of the bed profiler was ±1mm in the horizontal direction and ±0.5mm in the vertical direction. However even though the finger is very light it did cause a slight deformation (approximately 1-2mm) of the sand bed. This meant that the profiler tended to smooth out some of the finer features of the bed. Bed profiles were interpolated onto a regular spacing of 1mm.

Each test started from an initial slope of either 1:30 or 1:75 which was achieved using wooden templates installed on each side of the flume. The initial profile was then measured using the bed profiler.

Table 1: Sieve analysis of Redhill 110 sand

Percent by weight passing sieve			Soulsby
(%)	(mm)	(Phi)	ws (ms-1)
5	0.064	3.97	0.0026
10	0.074	3.75	0.0035
16	0.087	3.53	0.0048
25	0.095	3.40	0.0057
50	0.111	3.17	0.0077
75	0.135	2.89	0.0111
84	0.154	2.70	0.0141
90	0.167	2.58	0.0163
95	0.177	2.50	0.0180

Figure 1: Bed profiler and wave gauges 5 to 8

5. Test conditions

A total of 34 tests were performed. Details of the test conditions are given in Table II.

- Test type is either V = vertical, or S = sloping (1:2) with T added if the test had a varying water level;
- H_{si} is the measured incident offshore significant wave height (m) calculated by the least squares technique using gauges 1-4;
- T_p is the measured spectral peak wave period (s);
- h_t is the still water depth at the structure toe (m);
- Cr is the bulk reflection coefficient;
- S_t is the scour depth at the toe of the seawall (m) with negative values being accretion;
- S_{max} is the maximum scour depth (m);
- X_{sm} is the distance from the toe of the structure to the location of S_{max} (m);
- A_{max} is the maximum increase in bed level (m);
- X_{am} is the distance from the toe of the structure to A_{max} (m).

19 tests were performed with a vertical wall. 13 of these were with a beach slope of 1:30 and 6 were with a beach slope of 1:75. Details of these are given in Table 2. A total of 6 scour protection tests were carried out, but are not reported here. A sloping wall at 1:2 was used in 9 of the tests with a beach slope of 1:75.

The majority of tests used a constant incident significant wave height, period and depth to measure the time development of scour. In these tests a bed profile was taken before the test and after 300, 1000, and 3000 spectral peak wave periods. Scour and accretion results in Table II are presented after 3,000 peak wave periods.

In the second type (Tests 10, 17 and 34a) the water depth was varied to simulate part of a tidal cycle and in these tests a new profile was taken after each of the 300 wave bursts. Test 10 started with a water depth at the wall close to zero, increasing the depth in steps to a maximum depth of 0.3m then decreasing the depth in steps down to -0.1m at the seawall. However Test 17 started from a higher water depth of 0.2m and decreased the depth in steps down to -0.05m, while in Test 34a the water was slowly drained from the flume during the test. Table II gives results at the end of the test.

6. Bed level changes for a vertical wall

Bed level changes (final – initial elevation) at the end of Tests 7, 12, 4 and 11 (i.e. after 3,000 waves) are provided in Fig. 2. All the tests were performed with a vertical seawall. Negative values represent scour, while positive values represent accretion. These four tests had the same initial bed profile, wave period (T_p=3.24s) and incident wave height (H_s=0.2m) but different water depths (h_t=0.0m, 0.1m, 0.2m and 0.4m respectively). A comparison has been drawn between these four tests as they resulted in very different breaking wave conditions at the wall and hence different bed profiles.

During Test 7 (h_t=0.0m) the waves broke offshore and the wave energy was largely dissipated before the waves reached the wall in the swash zone. As a result there was a slight accretion at the wall but a general lowering throughout the rest of the profile. The vertical seawall was situated within the surf zone during Test 12 (h_t=0.1m) and some breaking occurred onto it, although most of the larger waves had already broken by the time they reached the seawall. The resulting scour profile includes a small dip at the toe of the seawall caused by turbulence and a deeper scour hole at about 0.5m from the structure toe.

However during Test 4 (h_t=0.2m) the waves tended to break onto the structure and the impacts sent water high up above the seawall (see Fig. 3). In these cases water plunging down the face of the seawall to the bed, resulted in suspended sediment transport at the toe, and this mechanism generated the deepest scour depths. Fig. 2 shows that the maximum scour occurred at the wall (0.158m) with significant accretion (0.056m) occurring 1.3m offshore.

In deeper water (Test 11, h_t=0.4m) the waves did not break onto the seawall as plunging breakers, but tended to reflect more energy. The scouring pattern (shown in Fig 2) in these cases was closer to the classic Xie type standing wave pattern. The maximum scour of 0.117m occurred away from the wall and was significantly less than the plunging breaker case shown in Fig. 2 (0.158m).

Table 2: Details of experiments performed

Test no.	Test type	Beach slope	H_{si} [m]	T_p (s)	H_t [m]	C_r [-]	S_t [m]	S_{max} [m]	X_{sm} [m]	A_{max} [m]	X_{am} [m]
1	V	1:30	0.193	1.55	0.200	0.50	0.057	0.057	0.031	0.006	0.660
2	V	1:30	0.193	1.87	0.200	0.49	0.065	0.065	0.031	0.023	0.680
3	V	1:30	0.198	2.29	0.200	0.47	0.130	0.130	0.031	0.044	0.950
4	V	1:30	0.194	3.24	0.200	0.46	0.158	0.158	0.031	0.056	1.369
5	V	1:30	0.197	4.58	0.200	0.44	0.140	0.143	0.049	0.073	2.449
6	V	1:30	0.204	1.87	0.000	0.09	-0.031	0.025	0.731	0.033	0.016
7	V	1:30	0.196	3.24	0.000	0.13	-0.011	0.032	1.513	0.026	0.082
8	V	1:30	0.197	1.87	0.100	0.26	0.110	0.111	0.006	0.009	0.731
9	V	1:30	0.202	1.87	0.400	0.82	-0.013	0.035	0.327	0.013	0.009
10	VT	1:30	0.195	1.87	-0.1 to 0.2	0.31	0.067	0.067	0.001	0.001	4.077
11	V	1:30	0.217	3.24	0.400	0.84	0.040	0.117	0.414	0.069	1.881
12	V	1:30	0.197	3.24	0.100	0.27	0.088	0.114	0.469	0.030	2.106
13	V	1:30	0.295	2.29	0.150	0.28	0.093	0.125	0.415	0.013	1.925
14	V	1:75	0.280	1.87	0.300	0.49	0.036	0.052	0.354	0.027	1.005
15	V	1:75	0.196	1.87	0.200	0.40	0.027	0.048	0.295	0.009	2.085
16	V	1:75	0.197	3.24	0.200	0.39	0.089	0.102	0.404	0.022	1.342
17	VT	1:75	0.193	1.87	0.2 to -0.1	0.16	0.014	0.034	0.191	0.004	3.617
18	V	1:75	0.191	4.58	0.200	0.37	0.062	0.119	0.495	0.055	2.662
19	V	1:75	0.215	3.24	0.400	0.77	0.050	0.100	0.417	0.067	1.901
26	S	1:75	0.190	1.87	0.200	0.31	0.063	0.068	0.165	0.010	4.590
27	S	1:75	0.192	3.24	0.200	0.36	0.104	0.105	0.232	0.024	3.729
28	S	1:75	0.194	1.55	0.200	0.28	0.062	0.072	0.155	0.009	3.565
29	S	1:75	0.241	1.87	0.300	0.49	0.063	0.052	0.203	0.014	3.232
30	S	1:75	0.243	3.24	0.400	0.64	0.043	0.064	0.124	0.055	3.652
31	S	1:75	0.201	1.87	0.000	0.07	-0.001	0.010	2.480	0.015	0.488
32	S	1:75	0.206	3.24	0.000	0.12	-0.006	0.023	2.640	0.068	0.069
33	S	1:75	0.192	1.87	0.400	0.50	0.014	0.024	0.066	0.014	3.384
34	S	1:75	≈0.20	3.24	0.100	-	0.069	0.079	0.201	0.006	2.682
34a	ST	1:75	≈0.20	3.24	0.1 to -0.1	-	0.074	0.081	0.210	0.002	2.642

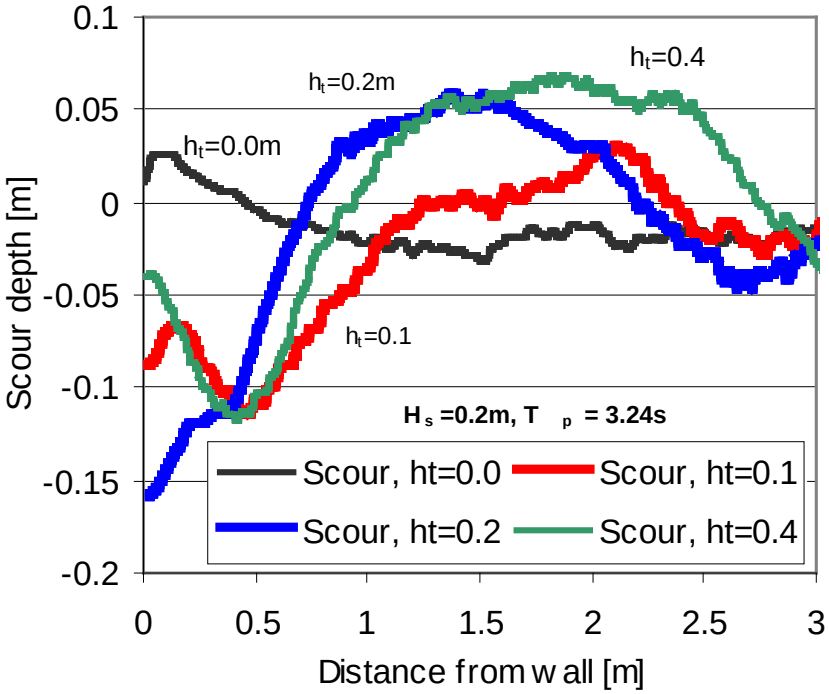

Figure 2: Bed level changes after tests 4, 7, 11 and 12

Figure 3: Wave breaking against a vertical wall. Metre stick for scale

7. Effect of beach slope

Four pairs of tests were performed where the same incident wave height, wave period, water depth and structure were used but in the first case the initial beach profile was at 1:30 while in the second case the initial beach slope was 1:75. The four pairs of tests were:

- 2 and 15 (H_{si}=0.19m, T_p=1.87s and h_t=0.20m);
- 4 and 16 (H_{si}=0.20m, T_p=3.24s and h_t=0.20m);
- 5 and 18 (H_{si}=0.19m, T_p=4.58s and h_t=0.20m);
- 11 and 19 (H_{si}=0.22m, T_p=3.24s and h_t=0.40m).

The scour depths for the 1:75 beach slope are plotted against the scour depths for the 1:30 beach in Fig. 4, which shows the toe scour depths and the maximum scour depths. It is clear that the 1:75 beach slope gave much lower scour depths than the 1:30 beach slope. Best-fit straight lines through the origin gave toe scour depths in the 1:75 beach as 52% of those in the 1:30 beach, while maximum scour depths were 75% of those in the 1:30 beach. The reason for this is believed to lie in the way the waves broke on the beach in front of the seawall.

The waves tended to break as spilling breakers on the 1:75 beach, where for the 1:30 case there were more breakers plunging onto the seawall causing turbulent jets to reach the seabed, resulting in scour.

8. Bed level changes for a sloping wall

Bed level changes (final – initial elevation) at the end of Tests 32, 27 and 30 (i.e. after 3,000 peak wave periods) are provided in Fig. 5. All the tests were performed with a 1:2 (V:H) smooth sloping seawall. Negative values represent scour, while positive values represent accretion. These three tests had the same initial bed profile, wave period (T_p=3.24s) and similar offshore incident wave height (H_s=0.19m to 0.24m) but different water depths (h_t=0.0m, 0.2m and 0.4m respectively). A comparison has been drawn between these three tests as they resulted in very different breaking wave conditions at the wall and hence different bed profiles.

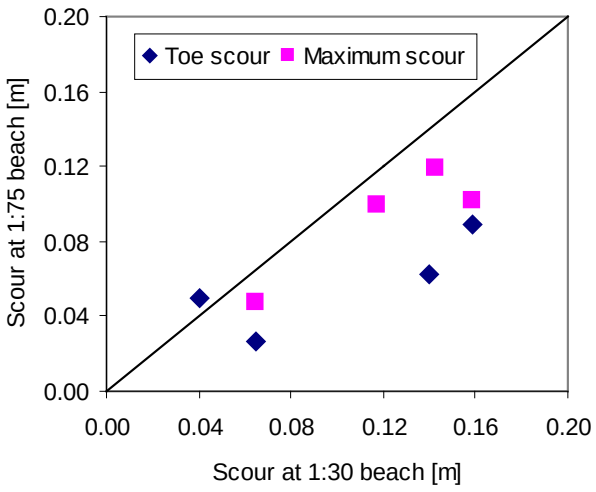

Figure 4: Scour depths in a 1:75 beach versus scour depths in a 1:30 beach

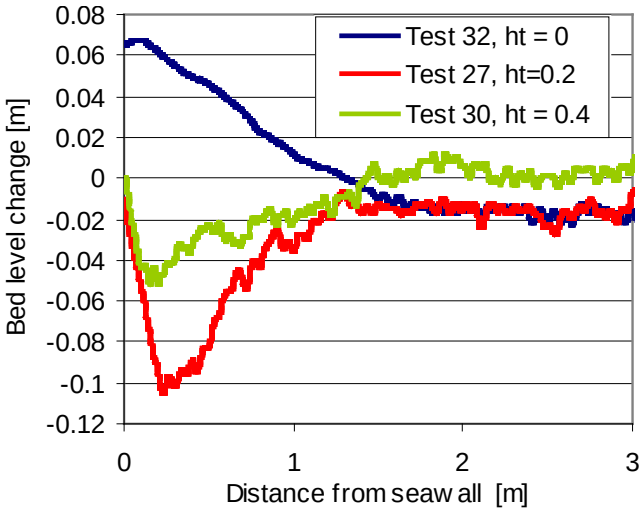

Figure 5: Bed level changes in front of a 1:2 sloping wall

The distance from the seawall is taken as the cross-shore distance from the point where the seawall emerged from the initial screeded bed profile. Test 32, with an initial toe depth of 0.0m again showed accretion. The largest scour depth again occurred for a toe depth of 0.2m (Test 27) while the scour depth for the higher toe depth of 0.4m (Test 30) was again lowered. In each of the latter two cases the initial part of the bed profile follows the line of the sloping seawall. Minor differences between the bed level changes from Tests 27 and 30 where both tests measured the sloping seawall are due to minor differences in the initial bed levels and to some small sand ripples that were left on the seawall at the end of the tests.

Three tests were performed with an incident significant wave height of 0.2m, peak period of 3.24s and water depth at the toe of 0.20m. These were Test 4 (vertical wall, 1:30 slope, S_t = 0.158m, S_{max} = 0.158m), Test 16 (vertical wall, 1:75 slope, S_t = 0.089m, S_{max} = 0.102) and Test 27 (sloping wall, 1:75 slope, S_t = 0.104m, S_{max} = 0.105m). This shows that reducing the initial beach slope reduced the toe and maximum scour depths. Changing the seawall from a vertical to a 1:2 slope increased the scour depths slightly. The differences between using a sloping and vertical seawall are investigated further in the next section.

9. Variation in scour depth with wall slope

Four pairs of tests were performed where the same incident wave height, wave period and water depth were used but in the first case a vertical wall was present while in the second case a sloping wall was present. In all cases an initial bed slope of 1:75 was used. The four pairs of tests were:

- 15 and 26 (H_{si}=0.20m, T_p=1.87s and h_t=0.20m);
- 16 and 27 (H_{si}=0.20m, T_p=3.24s and h_t=0.20m);
- 14 and 29 (H_{si}=0.26m, T_p=1.87s and h_t=0.30m);
- 19 and 30 (H_{si}=0.23m, T_p=3.24s and h_t=0.40m).

The sloping wall scour depth is plotted against the vertical wall scour depth in Fig. 6, for the scour depth at the structure toe and the maximum scour depth. The diagonal line plotted is the line of equivalence. Fig. 6 shows that for the four cases tested the scour depths were not, on average, reduced by replacing a vertical seawall with a 1:2 sloping seawall. This runs contrary to many people's expectations [1] that reducing the wall slope reduces the scour depth as it reduces the reflection coefficient (although the latter was observed).

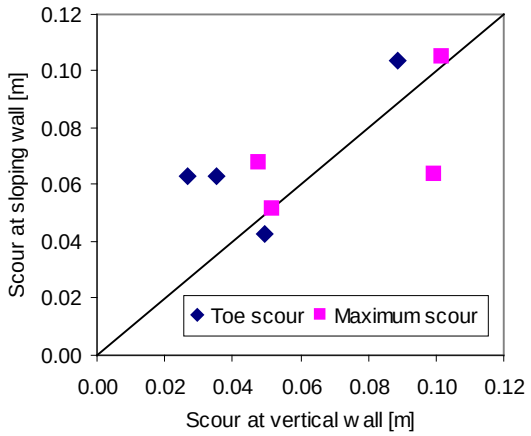

Figure 6: Scour depths at sloping wall versus scour depths at vertical wall. Diagonal line is line of equivalence

As with a vertical wall the scour depth reached partly depends on the way the wave runs down the seawall slope and interacts with the following wave. Deep scour depths appear to correlate well with wave run-down reaching the structure toe, which continued as a 1:2 slope under the beach.

10. Variation in scour depth with relative water depth

Fig. 7 shows the variation of relative scour depth, S/H_{si} with relative toe depth, h_t/L_p where $L_p = gT_p^2/(2\pi)$ is the deep water linear theory wavelength for the wave peak period, T_p at the toe depth h_t. Fig. 7 (top) shows the scour depth at the toe, S_t/H_{si} while Fig. 7 (below) shows the relative maximum scour depth, S_{max}/H_{si}. Fig. 7 shows the highest relative scour depth occurring for relative toe depth of $h_t/L_p \approx 0.01$ in both cases.

The trend of decreasing relative scour depths with increasing relative depth (for $h_t/L_p > 0.012$) fits with the form of the scour prediction formulae devised in [4] and [9] where measurements were made within this range. The trend of increasing relative scour depths for increasing relative depth (for $h_t/L_p < 0.012$) fits with the form of the scour prediction formulae devised in [3] where experiments showed increasing relative scour depths for $h_t/L_p \leq 0.015$. Some authors, such as [16] had considered that the variation of scour depth with relative depth in [3] ran contrary to expectations and other scour formulae.

These tests have reproduced the form of the results in [3] within the expected range. This illustrates the fact that scour occurs by different mechanisms in different hydrodynamic regimes. The different scouring mechanisms should not be expected to exhibit the same variation in scour depth with relative water depth. These tests have helped to reconcile the approaches of [3], [4] and [9].

Fig. 7 (left) shows that accretion occurred for the lowest and in one case for the highest relative water depths. Accretion occurred at the toe of the vertical structure for $h_t/L_p \approx 0$ due to swash zone processes.

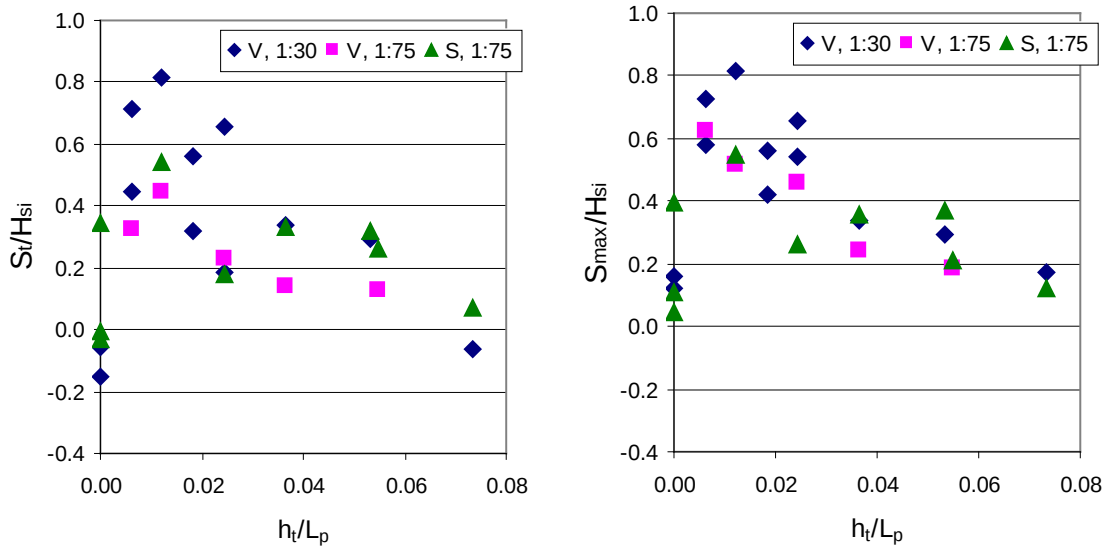

Figure 7: Variation of relative toe scour depth (left) and maximum scour depth (right) with relative toe depth

At high relative depths the lack of wave breaking resulted in a scouring pattern dominated by streaming and similar in form to those in [9]. In these cases accretion at the toe of the structure can occur.

Fig. 7 illustrates the differences between maximum and toe scour depths, which are shown over the same ranges and at the same scale to aid comparison. Maximum scour depths are all positive and are always larger than or equal to the toe scour depth. The maximum relative scour depth recorded was $S/H_s = 0.82$.

11. Variation in scour depth with Iribarren number

The observed dependency of the scour depth on the form of wave breaking on the structure indicates that there might be a relationship between scour depth and Iribarren number [17] (or surf similarity parameter as it is also known) defined in Equation 6 and including the beach slope, tan(α).

$$\mathrm{Ir} = \frac{\tan(\alpha)}{\sqrt{\mathrm{H_{si}}/\mathrm{L_p}}} \qquad (6)$$

On a uniformly sloping beach without a seawall the breaker type has been categorized as spilling for Ir < 0.5 and plunging for 0.5 < Ir < 3.3 [18] although there is no abrupt limit from one breaking state to the other for irregular waves. In this case the wave breaking in front of the structure was heavily influenced by the reflections from the structure (with reflection coefficient in excess of 0.8, see Table II). This has resulted in waves plunging onto the seawall for Iribarren numbers less than 0.5. Fig. 8 shows the variation of relative scour depth with Iribarren number for toe scour (top) and maximum scour (bottom).

There is a stronger apparent link between the relative maximum scour depth and Iribarren number than there is between the toe scour depth and the Iribarren number. A number of simple best-fit curves were calculated to show the link between relative maximum scour depth and Iribarren number. The simple linear fit given in (7) had the equal lowest mean absolute error of 0.134.

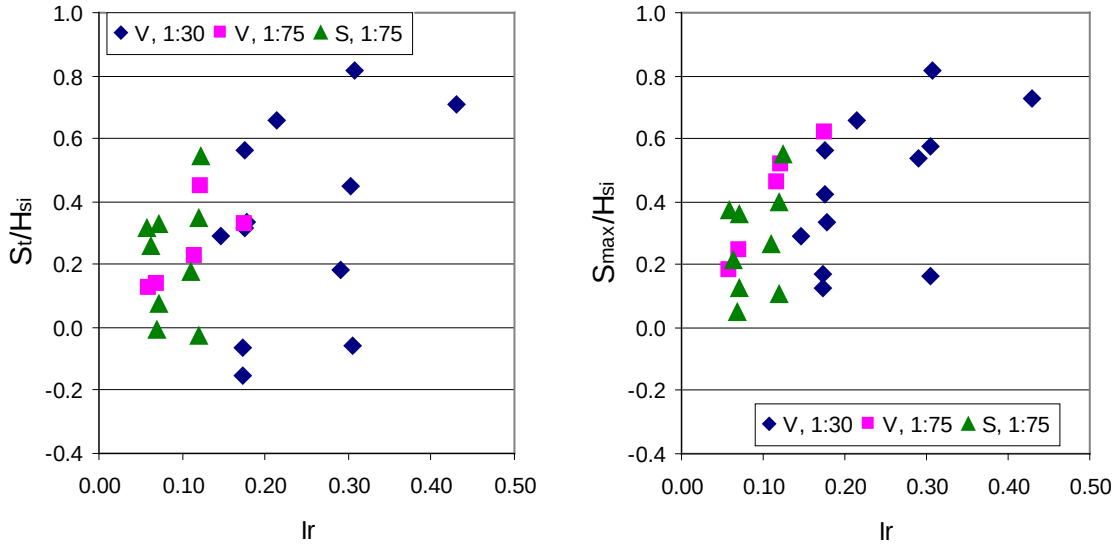

Figure 8: Variation of relative scour depth with Iribarren number for toe scour (left) and maximum scour (right)

$$\frac{S_{max}}{H_{si}} = 1.30 \times Ir + 0.169 \qquad (7)$$

However, there is a considerable variation in scour depths for similar values of Iribarren number. For example Tests 4, 7, 11 and 12 all have Iribarren numbers between 0.29 and 0.31 but have relative maximum scour depths between 0.16 and 0.82. All four tests have incident significant wave heights between 0.194m and 0.217m, peak periods of 3.24s and were performed with a vertical seawall and an initial beach slope of 1:30. The difference lies in the toe depth, which governs where the seawall is in relation to the position waves start to break and hence which hydrodynamic processes dominated. See Section VI for a discussion of these tests and Fig. 2 for their final bed profiles.

12. Variation of relative scour depth with Iribarren number and relative toe depth

Section X and XI have shown how scour depths vary with relative depth and Iribarren number. Fig. 9 shows relative scour depth plotted against relative toe depth, with the data arranged into three ranges of Iribarren number:

- Ir < 0.08;
- 0.1 < Ir < 0.2; and
- Ir > 0.2.

Fig. 9 shows that for any given relative depth, h_t/L_p, the greatest scour depths tend to occur for the larger Iribarren numbers. The trend appears more visibly obvious for the maximum scour depth than for the toe scour depth. This opens up the possibility of developing a scour predictor that is a function of relative toe depth and Iribarren number.

13. Ranges of parameters and logical limits to scour depth at high and low toe depths

The tests performed at HR Wallingford were within the following ranges:

1. $0.000 \leq h_t/L_p \leq 0.073$;
2. $0.059 \leq Ir \leq 0.430$;
3. $0.00 \leq h_t/H_{si} \leq 2.08$;
4. $0.006 \leq H_{si}/L_p \leq 0.052$;

Moreover, not all sections of these ranges were covered equally. Therefore, as with any set of experimental results, any extrapolation outside these limits (and for some cases within these limits) carries a risk. Nevertheless, some limits can be placed on the expected behaviour due to our understanding of the physical processes involved. If the beach extends above the maximum runup limit for a particular seastate, the waves will not reach the seawall so the scour depth at the wall is expected to be zero. Note however, that wave activity seawards of the beach toe may cause erosion that may, in time, extend to the seawall toe.

At the other extreme of very deep water the wave orbital velocity will tend towards zero and again no scour would be expected to occur. For relatively deep water and low (or flat) bed slopes accretion also occurs at the seawall for suspended load sediment transport [9].

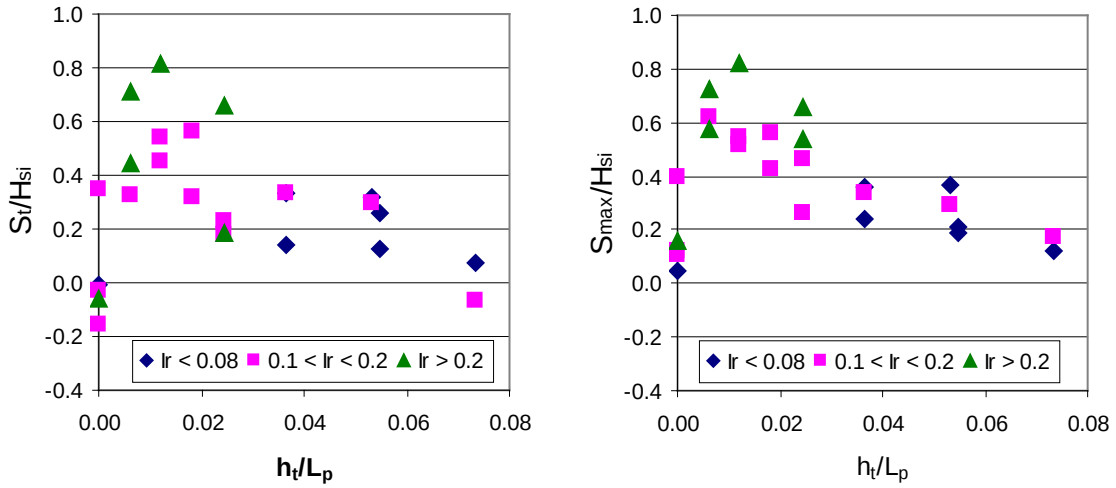

Figure 9: Variation of relative scour depth with relative toe depth for toe scour (left) and maximum scour (right)

14. Modelling of tidal half cycle

Measurements of toe scour at seawalls in the inter-tidal zone [19, 20, 21] show that scour holes can often form and refill within a single tide, leaving the beach level after the event similar to, or the same as, the beach level before the event. The full extent of such events cannot be determined from beach profiles measured at low tide.

Test 10 modeled a half tidal cycle using bursts of 300 peak wave periods at a series of discrete water levels, starting at 0.05m above the intersection of the vertical seawall and the initial 1:30 bed profile. The water level was then increased in steps of 0.05m to 0.30m before decreasing in steps of 0.05m to a level of -0.10m. Two additional bursts were then added, at levels of -0.08m and -0.09m to see if more infilling of the scour hole would occur.

The same offshore wave conditions were used for all water levels, with a target significant wave height of 0.20m, and spectral peak period of T_p = 1.87s. The gains on the wavemaker and the wave absorption system were tuned to the water depth before running each burst of waves to ensure that the offshore wave conditions were as uniform as possible.

The bed level change profiles from Test 10 are shown in Fig. 10, which is split into three sections. Fig. 10a shows the scour profiles from the rising water levels. The scour depth at the wall increased up until 1200 waves (with a water depth at the toe of 0.20m above the initial bed level) then decreased as the water level rose to 0.30m after 1800 waves. This is compatible with the results from Section VI and the observations that the greatest scour depths are achieved when waves break directly onto the seawall. This was observed to occur more at a depth of 0.20m than at higher or lower depths. The position of the maximum accretion (within 1.5m of the seawall) moves offshore from the seawall as the water depth and hence wavelength increases.

Fig. 10b shows the scour profiles from the greatest water depth of 0.30m (the last profile shown in Fig. 10a) down to a depth of 0.05m, after 3300 peak wave periods. Here the scour depth at the wall did not increase noticeably as the water level dropped from 0.30m to 0.20m, but it did increase as the water depth dropped from 0.20m to 0.10m. At the same time the location of maximum accretion (within 1.5m of the seawall) moved towards the seawall and decreased in elevation as the water level dropped, until after 3300 waves there was no accretion within 1.5m of the wall and the whole section of the seabed exhibited erosion. Between about 2m and 3m offshore a second area of accretion remained above the initial bed level.

Figure 10c shows the scour profiles from a water depth of 0.05m down to -0.10m then after 2 further bursts of waves at -0.08m and -0.09m. At these low water levels the further offshore mound (between 2m and 3m from the seawall) became gradually washed out and the bed profiles became smoother. The toe scour in front of the seawall also started to fill in by a small amount. The water depths for the final two bursts were chosen so that the offshore mound was just exposed as it seemed to be periodic swash events over this outer mound that contributed most to the infilling.

Figure 10c shows that the nearly complete infilling of scour holes seen in the field was only partially reproduced in the medium scale laboratory tests. Scale effects and the discrete representation of changes in water level as well as the longshore non-uniformity of bed levels are all likely to have contributed to the differences between the results in the laboratory and measurements made in the field.

15. Summary and Conclusions

A set of thirty-four medium-scale laboratory tests of toe scour at seawalls has been performed. The tests were all intended to generate suspended sediment transport within the laboratory flume and suspension was often observed during the tests. The tests were all carried out with irregular waves. The results are complementary to other medium-to-large scale laboratory tests that also used irregular waves, particularly 2 tests of [9], 1 of [13] and 18 of [3].

Two scour depths were determined: S_t the scour depth immediately adjacent to the toe of the structure and S_{max} the maximum scour depth measured at any point in the test section. Both are of interest in considering the stability of coastal structures. The presence of a deep scour hole at the toe of a structure may allow fill material to escape under the seawall, leaving a void behind the seawall that may cause its sudden collapse. A deep scour hole at the toe of the structure also means that the toe may slide outwards - another form of failure. A scour hole away from the structure toe is also of interest as its presence may shorten any slip surface, thereby increasing the risk of structural failure by sliding.

The relative scour depth was found to depend on the relative water depth at the structure toe, h_t/L_p and the Iribarren number (6). It was relatively insensitive to the slope of the seawall, with a 1:2 slope giving similar scour depths to a vertical seawall.

An attempt was made to reproduce the formation and in-filling of a scour hole during a half tidal cycle, as observed in the field. Only partial infilling occurred, probably as a result of scale effects and the discrete changes in water level made during the test.

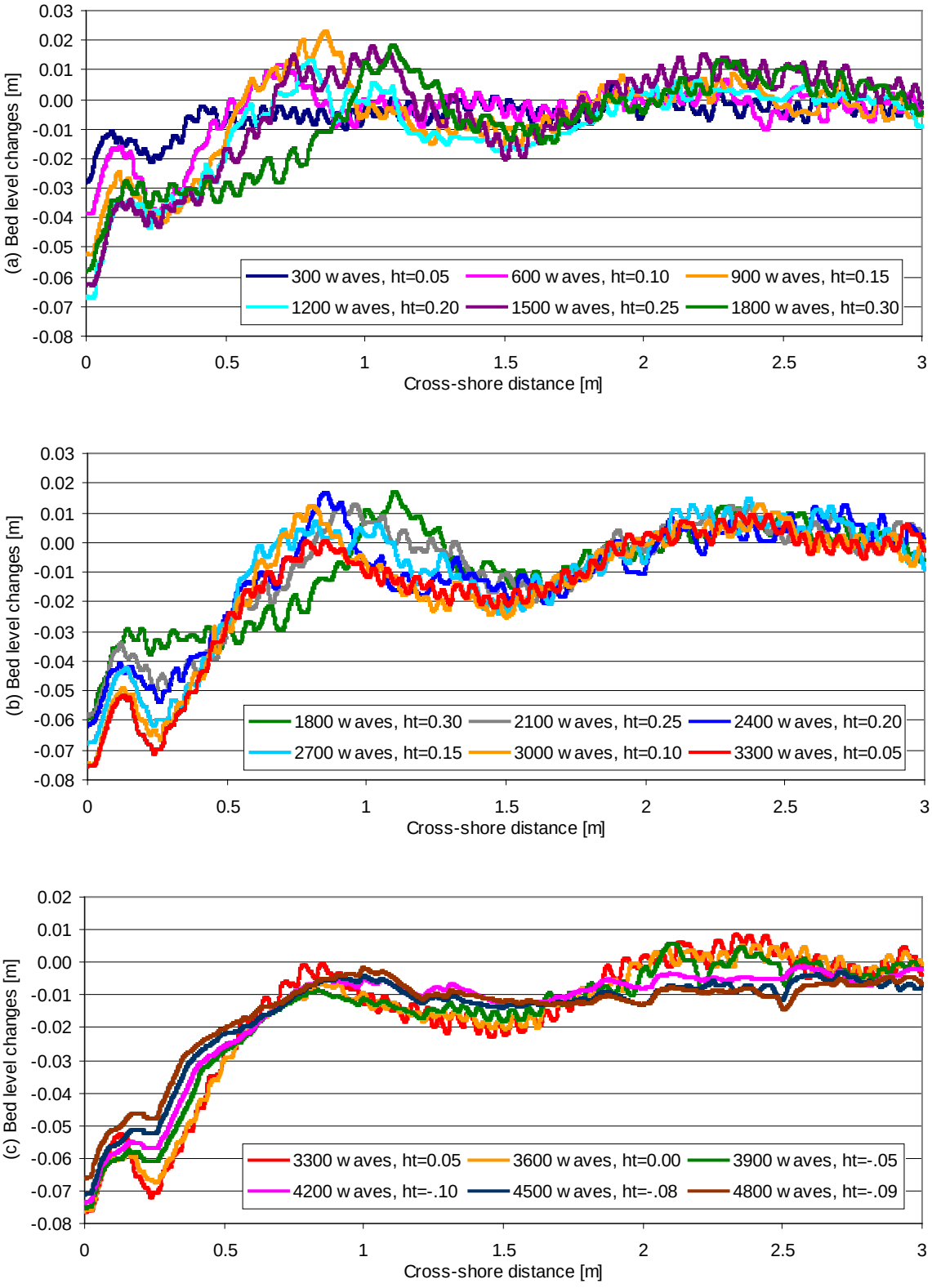

Figure 10: Bed level changes (from initial bed level) after a series of bursts of 300 waves at different levels to simulate half a tidal cycle

References

1. J. Sutherland, A. Brampton, G Motyka, B. Blanco and R. Whitehouse, Beach lowering in front of coastal structures. Research Scoping Study. Report FD1916/TR1, 2003. INTERNET: available from http://sciencesearch.defra.gov.uk/ (page accessed 05/04/06).
2. B.M. Sumer and J. Fredsøe, The mechanics of scour in the marine environment. World Scientific, 2002, pp.536.
3. J.E. Fowler, Scour problems and methods for prediction of maximum scour at vertical seawalls. Technical Report CERC-92-16, U.S. Army Corps of Engineers, Waterways Experiment Station, 3909 Halls Ferry Road, Vicksburg, MS, 1992.
4. B.M. Sumer and J. Fredsøe, Experimental study of 2D scour and its protection at a rubble-mound breakwater. Coastal Engineering, vol 40, pp. 5-87, 2000. Elsevier Science.
5. Irie and K. Nadaoka, Laboratory reproduction of seabed scour in front of breakwaters. *Proc 19th Int Conf on Coastal Engineering*, Houston. ASCE, pp. 1715-1731, 1984.
6. J.W. Kamphuis, On understanding scale effect in coastal mobile bed models. In *Physical Modelling in Coastal Engineering*, AA Balkema, Rotterdam, pp. 141-162, 1985.
7. R.G. Dean, Physical modelling of littoral processes. In *Physical Modelling in Coastal Engineering*, AA Balkema, Rotterdam, pp. 119-139, 1985.
8. S.A. Hughes and J.E. Fowler, *Midscale physical model validation for scour at coastal structures*. Technical Report CERC-90-8, US Army Corps of Engineers, CERC, Vicksburg, Miss., 1990.
9. S-L. Xie, *Scouring patterns in front of vertical breakwaters and their influence on the stability of the foundations of the breakwaters.* Department of Civil Engineering, Delft University of Technology, Delft, The Netherlands, 61p. 1981.
10. R.L. Soulsby, *Dynamics of Marine Sands.* Thomas Telford, London. ISBN 07277 2584 X, 1997.
11. P.D. Komar and M.C. Miller, Sediment threshold under oscillatory water waves. *J. Sediment. Petrol.* Vol 43, pp. 1101-1110, 1974.
12. N.C. Kraus, J.M. Smith and C.K. Sollitt, SUPERTANK Laboratory Data Collection Project, *Proc 23rd Int Conf on Coastal Engineering*, American Society of Civil Engineers, pp 2191 – 2204, 1992.
13. N.C. Kraus and J.M. Smith (editors), *SUPERTANK Laboratory data collection project. volume 1: Main text*. Technical report CERC-94-3, US Army Corps of Engineers Waterways Experiment Station, Coastal Engineering Research Center, Vicksburg. Miss., 1994.
14. HR Wallingford, *Design of physical model scour tests*. HR Wallingford Technical Note CBS0726/02, 2005.
15. HR Wallingford, *Medium scale 2D physical model tests of scour at seawalls*. HR Wallingford Technical Note CBS0726/06, 2006.
16. W.G. McDougal, N. Kraus and H. Ajiwibowo, The effects of seawalls on the beach Part 2: numerical modeling of SUPERTANK seawall tests. *Journal of Coastal Research* Vol 12(3) pp. 702 – 713, 1986.
17. J.A. Battjes, Surf similarity. *Proceedings of the 14th Int Conf on Coastal Engineering*, ASCE, pp. 466-480, 1974.
18. J.M. Smith, Surf zone hydrodynamics. Part 2, Chapter 4 of the *Coastal Engineering Manual*, USACE EM 1110-2-1100, 2003.
19. J. Sutherland and A.M.C. Pearce, *Beach lowering and recovery at Southbourne (2005*). HR Wallingford Technical Note CBS0726/01, 2006.

20. HR Wallingford, *Scour monitor deployment at Blackpool*. HR Wallingford Technical Note CBS0726/04, 2005.
21. A.M.C. Pearce, J. Sutherland, G. Müller, D. Rycroft and R.J.S. Whitehouse, Scour at a seawall – field measurement and physical modeling. In Proc *30th Int Conf Coastal Engineering 2006*. San Diego, USA. World Scientific, pp 2378 – 2390